



## Three-Phase Inverter Control by Model Predictive Control

Arash Ahmadi, MohammadJavad Ahmadifar\*, Sobhan Ahmadi

Department of Electronics, Kermanshah Science and Research branch, Islamic Azad university, Kermanshah, IRAN

Available online at: [www.isca.in](http://www.isca.in), [www.isca.me](http://www.isca.me)

Received 11<sup>th</sup> September 2013, revised 13<sup>th</sup> January 2014, accepted 20<sup>th</sup> April 2014

### Abstract

*The present study used a model predictive control (MPC) as internal current controller of a PV system. An external voltage controller with PI controller were used to control the terminal voltages of a PV system to track MPP. Due to its high flexibility, the MPC controller well perform as internal controller in definition of cost function. In MPC controller, the reference current tracks the reference current by fast dynamic without ultra-mutation.*

**Keywords:** Distributed production source, model predictive control (MPC), resonant control (PR).

### Introduction

Due to the lack of fossil fuel resources and environmental issues arising from this type of fuel, renewable energy sources has been interested by many researchers. One of the most popular renewable energy sources is photovoltaic (PV) system which can be used due to advances in technology and lower prices for solar panels. Due to recent advances in power converters interface these resources and network, also, flexibility of these resource has increased. One of the most important issues regarding control of PV systems is to use maximum power of the system under different solar radiations and surface temperatures of these sources. Therefore, operating point is always set at the maximum power point (MPP) by terminal voltage control of PV panels. For the terminal voltage control of PV systems, an internal loop controller and an external voltages controller are needed, to regulate the current and to set the voltage of PV panels, respectively. There are many methods investigated to design internal current controller. The state feedback approach described in carpita et al.<sup>1</sup> has a fast dynamic response to load changes. However, it is necessary to calculate duty ratio of switches in each switching period. Hysteresis control method is based on current control as internal loop control for voltage controller or as external controller for applications such as motor control. In this method, reference current is controlled directly by switch status; thus, a controller is not linear and definitions like phase limit and gain are not directly applicable. In addition to these two methods which are the most common control methods, more advanced controllers with particular properties have been developed. Advances in microprocessors lead to increasing advances in their application. Deadbeat control method is well able to track the reference voltage; however, it extremely needs the output filter information of the inverter<sup>2</sup>. Discrete time sliding mode control is able to track reference signal quickly. Its advantage is that the response is ultra-mutative. Furthermore, this controller is resistance to different load or network conditions and its efficiency less declines<sup>3,4</sup>. In predictive control, system stability increases and

the reference signal is tracked correctly. However, it is necessary to know exact values of systemic parameters to predict the response.  $H_{\infty}$  control method provides a resistant controller against different conditions; moreover, it does not need to know the exact model of the system. However, this controller weakly performs for nonlinear loads<sup>5</sup>. The present study used a model predictive controller (MPC) as internal current controller<sup>6-10</sup> and a PI controller as external voltage controller in synchronous rotating reference frame to set voltage of PV panel to work in MPP<sup>11-13</sup>. PI controller is able to track reference value of DC quantities with zero error. Its adjustment allows achieving a proper dynamic. The internal MPC is also a fast controller without ultra-mutation. It is able to implement some protective restrictions including protection against over current. Section 2 describes a PV system. Section 3 explains MPC current controller and section 4 introduces problems related to external voltage controller which is simulated in section 5 by MATLAB/Simulink.

### PV System

The relation of the current voltage is a nonlinear relation in a solar cell as shown in Figure 1. This heavily depends on radiation and temperature of the cell. Increased radiation increases short circuit current and the cell is able to generate more power. Increased temperature reduces open circuit voltage of the cell and decreases generated power. Figure 1 shows current voltage curve for different loads. To achieve high-level voltage, some PV panels are serried together. As many solar panels are serried, voltage increases. This prevents providing a good current. Therefore, the serried panels become parallel to allow more current with less voltage loss. By removal of each parallel panel, other panels can continue their work.

The power generated by a solar cell is equal to product of current multiplied in voltage. Figure 2 shows voltage power curve for solar cell. Under certain radiation and temperature, value of generated power is not equal in different working

points. Thus, systemic working point becomes constant on MPP for an efficient system. Therefore, it is necessary to maximize systemic working point to achieve maximum power. Maximum power is tracked by setting output voltage of panels.

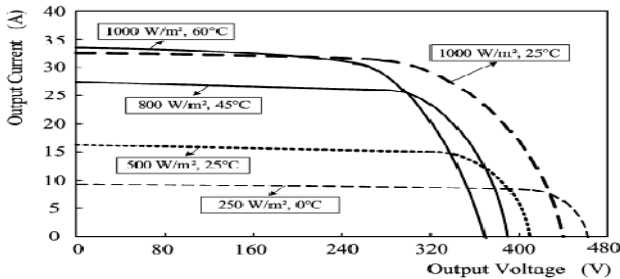


**Figure-1**  
Current voltage curve of a solar panel under different temperatures and radiations

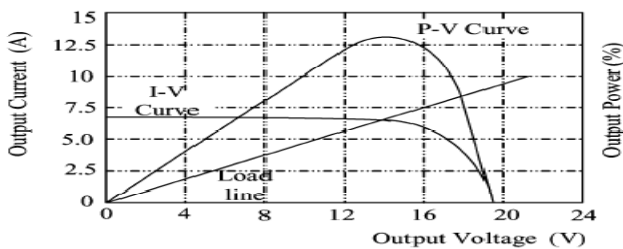


**Figure-2**  
Power voltage curve

### MPC Controller as Internal Current Controller

Figure 3 shows the controlled system.

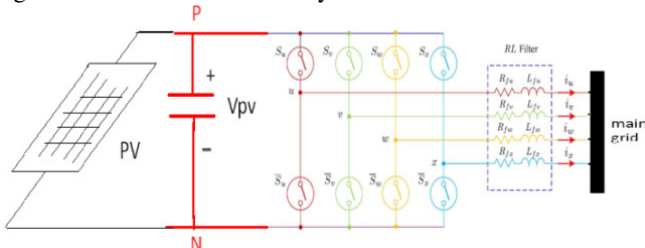


**Figure-3**  
The studied PV system

The mathematical model of the system is initially obtained to design and implement controller. For control signals  $S_u, S_v, S_w, S_x$  generate totally  $2^4$  different switching vectors for the four-leg inverter. When  $S_i$  is 1, the switch over the  $i$ th leg ( $i = u, v, w$ ) turns on. Under this condition, voltage of each phase to the point N which is negative terminal of the voltage is calculated as follows:

$$\begin{bmatrix} v_{uN} \\ v_{vN} \\ v_{wN} \\ v_{xN} \end{bmatrix} = \begin{bmatrix} S_u \\ S_v \\ S_w \\ S_x \end{bmatrix} \cdot v_{pv} \quad (1)$$

The (1) can be rewrite as follows:

$$v_{jN} = S_j v_{pv}, j = u, v, w, x. \quad (2)$$

The voltage applied to the output filter is describes in terms of the considered voltages, as follows:

$$\begin{bmatrix} v_{ux} \\ v_{vx} \\ v_{wx} \end{bmatrix} = \begin{bmatrix} S_u - S_x \\ S_v - S_x \\ S_w - S_x \end{bmatrix} \cdot v_{pv} \quad (3)$$

The (3) can be simplified as follows:

$$v_{yx} = v_{yN} - v_{xN} = (S_y - S_x) \cdot v_{pv}, y = u, v, w. \quad (4)$$

Thus, inverter voltages are obtained by following equations:

$$\begin{bmatrix} v_{uN} \\ v_{vN} \\ v_{wN} \\ v_{xN} \end{bmatrix} \begin{bmatrix} R_{fu} & 0 & 0 & 0 \\ 0 & R_{fv} & 0 & 0 \\ 0 & 0 & R_{fw} & 0 \\ 0 & 0 & 0 & R_{fx} \end{bmatrix} \begin{bmatrix} i_u \\ i_v \\ i_w \\ i_x \end{bmatrix} + \begin{bmatrix} L_{fu} & 0 & 0 & 0 \\ 0 & L_{fv} & 0 & 0 \\ 0 & 0 & L_{fw} & 0 \\ 0 & 0 & 0 & L_{fx} \end{bmatrix} \frac{d}{dt} \begin{bmatrix} i_u \\ i_v \\ i_w \\ i_x \end{bmatrix} + \begin{bmatrix} 1 \\ 1 \\ 1 \\ 1 \end{bmatrix} \cdot v_{nN} \quad (5)$$

which can be rewritten as follows:

$$v_{jN} = (R_{fj})i_j + L_{fj} \frac{di_j}{dt} + v_{nN}, j = u, v, w, x. \quad (6)$$

Current derivation of equation (5) was isolated as follows:

$$\frac{di_j}{dt} = \frac{1}{L_{fj}} [(v_{jN} - v_{nN}) - (R_{fj}) \cdot i_j], j = u, v, w, x \quad (7)$$

Based on (2) and (6), voltage of inverter neutral point is calculated as follows:

$$v_{nN} = L_{eq} \cdot v_{DC} \sum_{k=u,v,w,x} \frac{S_k}{L_{fk}} - L_{eq} \sum_{k=u,v,w,x} \frac{R_{fk}}{L_{fk}} i_k \quad (8)$$

$$\text{Where, } L_{eq} = \left( \frac{1}{L_{fu}} + \frac{1}{L_{fv}} + \frac{1}{L_{fw}} + \frac{1}{L_{fx}} \right)^{-1} \quad (9)$$

$$i_u + i_v + i_w + i_x = 0. \quad (10)$$

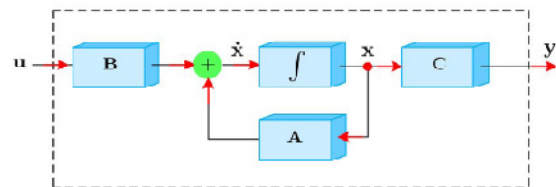


**Figure-4**  
Block diagram of three-phase four-leg inverter mode equations

State space model of the system is calculated as follows:

$$\begin{aligned} \dot{x} &= Ax + Bu \\ y &= Cx \end{aligned} \quad (11)$$

$$\begin{aligned} \text{Where: } x &= [x_1 x_2 x_3]^T = [i_u i_v i_w]^T \\ u &= [u_1 u_2 u_3]^T = [v_{ux} v_{vx} v_{wx}]^T. \end{aligned} \quad (12)$$

Figure-4 shows block diagram of (11). Matrix value of A, B and C are obtained by (5). Matrix values of A and B are shown in appendix and C is a unit 3x3 matrix.

Figure-5 shows the simplified model of the controller. As explained before, predictive controller is based on minimized cost function of the next period of sampling. The discrete time model was used to predict the next sample.

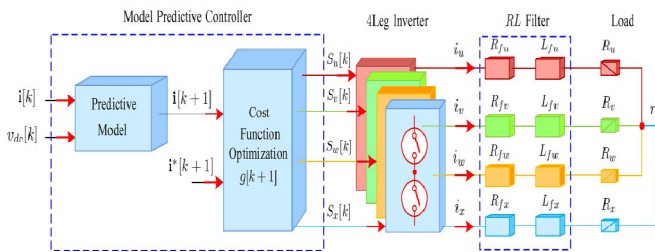


Figure-5

**Predictive control scheme for a three-phase 4-leg Inverter**

**Measured reference values:** reference values and some value of the system are measured to predict the model for inverter current control. Values and voltage of DC link and inverter output current are used as measured variables and value of reference current is defined from fourth-order extrapolation Lagrange:

$$i^*[k + 1] = 4i^*[k] - 6i^*[k - 1] + 4i^*[k - 2] - i^*[k - 3] \quad (13)$$

The above equation can be used for a wide frequency range of reference current. Extrapolation is not needed where the sampling interval  $T_s$  is too small.

**Predictive model:** to control the system, it is necessary to use system model to predict current value in the future. Regarding discrete control system, it is necessary to model the system in discrete mode. The discrete system model involves a recursive matrix which allows model prediction. That is, it is possible to predict mode variables in  $(k + 1)T_s$  by knowing values of control signal and mode in the instant  $T_s$ . Based on (11), the recursive matrix is shown as (14).

$$i[k + n + 1] = Fi[k + n] + Gu[k + n], n = 0, 1, 2, \dots \quad (14)$$

$$\text{where, } F = \begin{bmatrix} f_1 & f_2 & f_3 \\ f_4 & f_5 & f_6 \\ f_7 & f_8 & f_9 \end{bmatrix} = e^{AT_s} \quad (15)$$

$$G = \begin{bmatrix} g_1 g_2 g_3 \\ g_4 g_5 g_6 \\ g_7 g_8 g_9 \end{bmatrix} = A^{-1}(F - I_{3 \times 3})B.$$

**Optimizing cost function:** cost function which is related to reference value of future time is minimized by a proper stimulation in the final stage.

To select the proper switching vector,  $i_{[k+1]}$  is calculated from 16 switching vectors; the vector which generates the lowest cost function regarding the next reference current is not selected. The cost function  $g$  is defined as follows:

$$\begin{aligned} g[k + 1] &= ||i^*[k + 1] - i[k + 1]||^2 \\ &= (i_u^*[k + 1] - i_u[k + 1])^2 + (i_v^*[k + 1] - i_v[k + 1])^2 + (i_w^*[k + 1] - i_w[k + 1])^2 \end{aligned} \quad (16)$$

When the current reaches to reference current, the function  $g$  will be zero.

To optimize, these 16 switching vectors were calculated. The vector with the lowest cost function was selected regarding next reference current.

Figure 6 shows flowchart of a control algorithm.

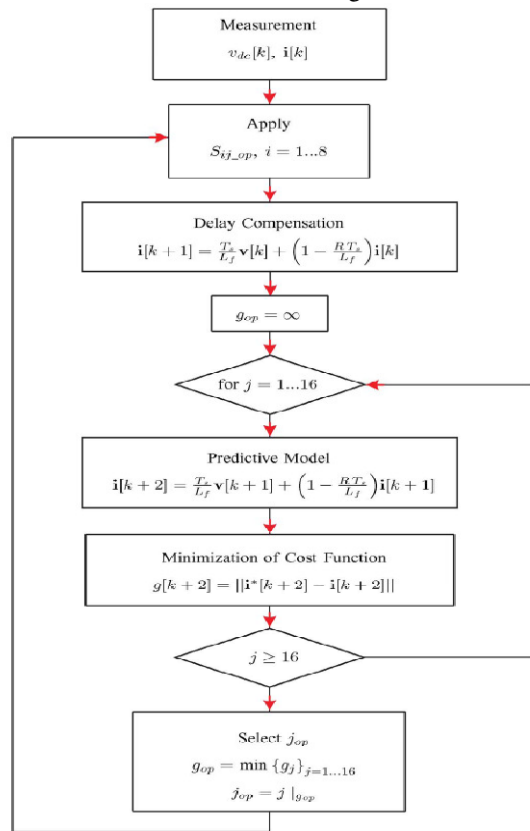


Figure-6  
MPC flowchart

### Output Voltage Controller

To set terminal voltages of PV system, an external controller, PI, was used. Therefore, AC variables were initially defined in synchronous rotating frame to convert them to DC variables by (17) where  $\omega t$  is synchronous frame of reference phase.

$$\begin{bmatrix} V_a \\ V_b \\ V_c \end{bmatrix} = \begin{bmatrix} \sin(\omega t) & \cos(\omega t) & 1 \\ \sin(\omega t - 120) & \cos(\omega t - 120) & 1 \\ \sin(\omega t + 120) & \cos(\omega t + 120) & 1 \end{bmatrix} \cdot \begin{bmatrix} V_d \\ V_q \\ V_0 \end{bmatrix} \quad (17)$$

Because control variables are totally DC, PI can track reference values by proper dynamic and zero stable error. Figure 7 shows control diagram of this method. Direction of PV voltage control is used from  $I_d$  current which is an active element of the current.

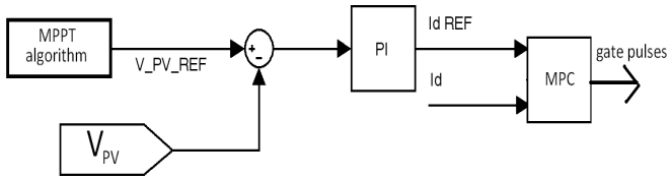


Figure-7  
 Diagram block of PV voltage controller

If the power generated by PV is more than the power transmitted to network, the additional generated power will be saved in the capacitor resulting in increased capacitor voltage. When the power injected to the network by the inverter is more than the power generated by PV panel, the capacitor voltage will be decreased. Thus, it is necessary to increase the active current value injected to network in order to decrease voltage. It is also required to decrease active power transmitted to network to charge the capacitor in a higher voltage level. Therefore,  $I_d$  current value which is an active element of the current inversely influences on increase of decrease in voltage. Thus, it is required to select negative coefficients of PI controller. When using voltage phase of the network as synchronous reference frame phase, voltage  $V_q$  of the network is zero and active and reactive powers transmitted to the network are calculated by (18) and (19).

$$P = \frac{3}{2} V_d \cdot I_d \quad (18)$$

$$Q = \frac{3}{2} V_d \cdot I_q \quad (19)$$

In PV voltage controller,  $I_d$  is generated by voltage controller and set in a certain level to adjust the capacitor voltage. In fact, the controller equals the generated power and injected power by  $I_d$ . Value of the reactive power injected to the network is calculated by equation 19. Thus,  $I_d$  can determine value of the reactive power injected to the network.

### Simulation and Test

This section simulated a PV system connected to three-phase

network by a four-leg inverter to support the system. Simulation was conducted by MATLAB/Simulink in which the network was a four-wire three-phase network with phase-to-phase voltage (120v). Value of reference voltage was first calculated for the PV system by MPPT algorithm as 250v. As Figure 8 shows, the system started to work from zero; capacitor voltage was finally constant in 250v. Figure 9 also shows the current injected to the network.

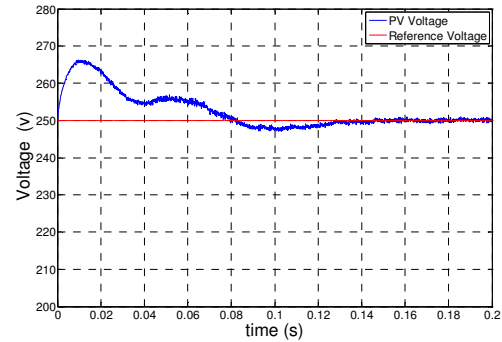


Figure-8  
 Voltage of the capacitor connected to PV during startup from zero

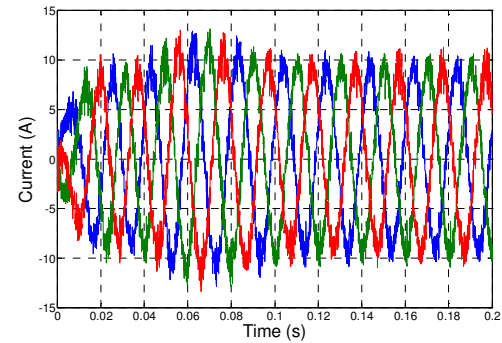


Figure-9  
 Current of phases a, b, c

Figure-10 shows variations of PV reference voltage from 250v to 200v and again to 250v. Figures-11, 12 and 13 show PV current as well as active power and current injected to the network, respectively.

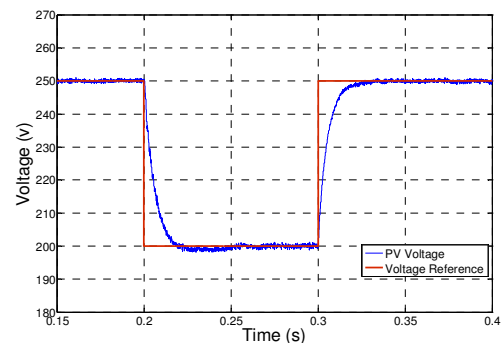
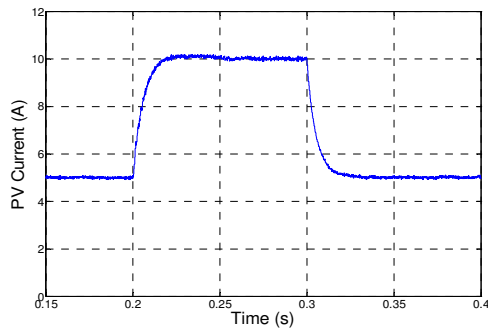
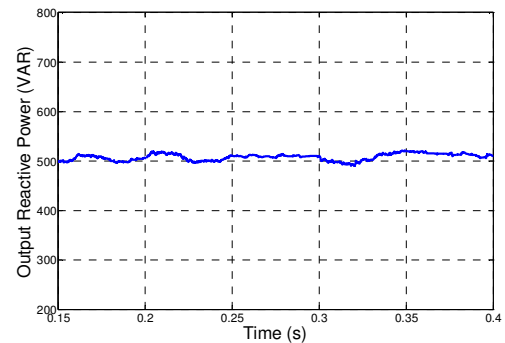


Figure-10  
 Reference voltage tracking of PV panel terminal



**Figure-11**

**Variations of PV panel current during changes in reference voltage**



**Figure-14**

**Variations of reactive power during changes in active power**

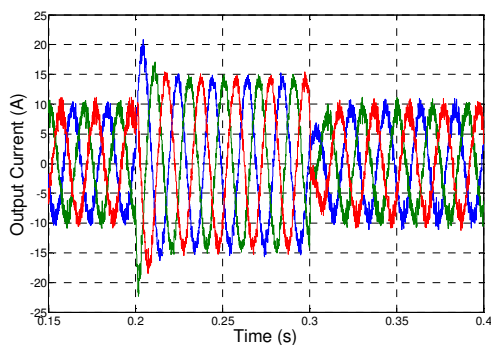


**Figure-12**

**Variations of output current during changes in reference voltage**

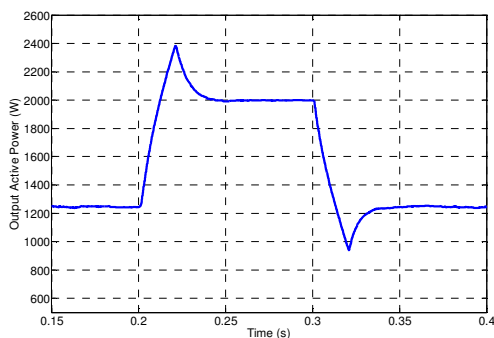


**Figure-13**

*Variations of output active power during changes in reference voltage*

During variations of active power (figure-14) reference value of reactive power (500 VAR) does not change.

## Conclusion

Predictive controller is able to track any kinds of currents due to its fast dynamic response and high flexibility. Therefore, it well performs as internal controller. The performance of this controller was supported as internal controller in a PV system with external voltage controller to run MPPT algorithm.

## References

1. Carpita M., Mazzucchelli M., Savio S. and Sciutto G., A new PWM control system for UPS using hysteresis comparator, In *IEEE Industry Applications Conference Ann. Meeting, San Diego, CA, 749-754 (1987)*
2. Kawabata T., Miyashita T. and Yamamoto Y., Dead beat control of three phase PWM inverter, *Power Electronics, IEEE Transactions on*, **5(1)**, 21-28 (1990)
3. Buso S., Fasolo S. and Mattavelli, P., Uninterruptible power supply multiloop control employing digital predictive voltage and current regulators, *Industry Applications, IEEE Transactions on*, **37(6)**, 1846-1854 (2001)
4. Siew-Chong tan, Yuk- Ming Lai and Chi Kong Tse, Sliding Mode Control of Switching Power Converters: Technique and Implementation, CRC Press, Taylor and Francis Group, (2012)
5. Lee T.S., Chiang S.J. and Chang J.M., H loop-shaping controller designs for the single-phase UPS inverters, *Power Electronics, IEEE Transactions on*, **16(4)**, 473-481 (2001)
6. Cortés P., Kazmierkowski M.P., Kennel R.M., Quevedo D.E. and Rodríguez J., Predictive control in power electronics and drives, *Industrial Electronics, IEEE Transactions on*, **55(12)**, 4312-4324 (2008)
7. Kennel R., Linder A. and Linke M., Generalized predictive control (GPC)-ready for use in drive applications?, In *Power Electronics Specialists Conference, 2001. PESC. 2001 IEEE 32nd Annual*, **4**, 1839-1844 (2001)
8. Yang S.M. and Lee C.H.A, Deadbeat current controller for field oriented motor drives, *Power Electronics, IEEE Transactions on*, **17(5)**, 772-778 (2002)
9. Abu-Rub H., Guzinski J., Krzeminski Z. and Toliyat H.A., Predictive current control of voltage source

inverters. In *Industrial Electronics Society, 2001. IECON'01. The 27th Annual Conference of the IEEE. 2*, 1195-1200 (2001)

10. Bode G.H., Loh P.C., Newman M.J. and Holmes D.G., An improved robust predictive current regulation algorithm, *Industry Applications, IEEE Transactions on*, **41(6)**, 1720-1733 (2005)
11. Malesani L., Mattavelli P. and Buso S., Robust dead-beat current control for PWM rectifiers and active filters, In *Industry Applications Conference, Thirty-Third IAS Annual Meeting, The 1998 IEEE.*, **2**, 1377-1384 (1998)
12. Espi Huerta J.M., Castello-Moreno J., Fischer J.R. and García-Gil R., A synchronous reference frame robust predictive current control for three-phase grid-connected inverters, *Industrial Electronics, IEEE Transactions on*, **57(3)**, 954-962 (2010)
13. Kouro S., Cortés P., Vargas R., Ammann U. and Rodríguez J., Model predictive control—A simple and powerful method to control power converters, *Industrial Electronics, IEEE Transactions on*, **56(6)**, 1826-1838 (2009)

### Appendix

$$A = \begin{bmatrix} a_1 & a_2 & a_3 \\ a_4 & a_5 & a_6 \\ a_7 & a_8 & a_9 \end{bmatrix}$$

$$a_1 = -\frac{R_{fu}}{L_{fu}} + \frac{L_{eq}}{L_{fu}} \left( \frac{R_{fu}}{L_{fu}} - \frac{R_{fx}}{L_{fx}} \right)$$

$$a_2 = \frac{L_{eq}}{L_{fu}} \left( \frac{R_{fv}}{L_{fv}} - \frac{R_{fx}}{L_{fx}} \right)$$

$$a_3 = \frac{L_{eq}}{L_{fu}} \left( \frac{R_{fw}}{L_{fw}} - \frac{R_{fx}}{L_{fx}} \right)$$

$$a_4 = \frac{L_{eq}}{L_{fv}} \left( \frac{R_{fu}}{L_{fu}} - \frac{R_{fx}}{L_{fx}} \right)$$

$$a_5 = -\frac{R_{fv}}{L_{fv}} + \frac{L_{eq}}{L_{fv}} \left( \frac{R_{fv}}{L_{fv}} - \frac{R_{fx}}{L_{fx}} \right)$$

$$a_6 = \frac{L_{eq}}{L_{fv}} \left( \frac{R_{fw}}{L_{fw}} - \frac{R_{fx}}{L_{fx}} \right)$$

$$a_7 = \frac{L_{eq}}{L_{fw}} \left( \frac{R_{fu}}{L_{fu}} - \frac{R_{fx}}{L_{fx}} \right)$$

$$a_8 = \frac{L_{eq}}{L_{fw}} \left( \frac{R_{fv}}{L_{fv}} - \frac{R_{fx}}{L_{fx}} \right)$$

$$a_9 = -\frac{R_{fw}}{L_{fw}} + \frac{L_{eq}}{L_{fw}} \left( \frac{R_{fw}}{L_{fw}} - \frac{R_{fx}}{L_{fx}} \right)$$

$$B = \begin{bmatrix} b_1 & b_2 & b_3 \\ b_4 & b_5 & b_6 \\ b_7 & b_8 & b_9 \end{bmatrix}$$

$$b_1 = \frac{v_{dc}}{L_{fu}} \left( 1 - \frac{L_{eq}}{L_{fu}} \right)$$

$$b_2 = -\frac{v_{dc}}{L_{fu}} \frac{L_{eq}}{L_{fv}}$$

$$b_3 = -\frac{v_{dc}}{L_{fu}} \frac{L_{eq}}{L_{fw}}$$

$$b_4 = -\frac{v_{dc}}{L_{fv}} \frac{L_{eq}}{L_{fu}}$$

$$b_5 = \frac{v_{dc}}{L_{fv}} \left( 1 - \frac{L_{eq}}{L_{fv}} \right)$$

$$b_6 = -\frac{v_{dc}}{L_{fv}} \frac{L_{eq}}{L_{fw}}$$

$$b_7 = -\frac{v_{dc}}{L_{fw}} \frac{L_{eq}}{L_{fu}}$$

$$b_8 = -\frac{v_{dc}}{L_{fw}} \frac{L_{eq}}{L_{fv}}$$

$$b_9 = \frac{v_{dc}}{L_{fw}} \left( 1 - \frac{L_{eq}}{L_{fw}} \right)$$